Scanning Microscopy

Volume 2 | Number 2 Article 17

11-23-1987

Transit Time Effect on Voltage Contrast in the Stroboscopic Scanning Electron Microscope

K. Nakamae
Osaka University

H. Fujioka
Osaka University

K. Ura
Osaka University

Recommended Citation

Nakamae, K.; Fujioka, H.; and Ura, K. (1987) "Transit Time Effect on Voltage Contrast in the Stroboscopic Scanning Electron Microscope," *Scanning Microscopy*: Vol. 2 : No. 2 , Article 17.
Available at: https://digitalcommons.usu.edu/microscopy/vol2/iss2/17

Scanning Microscopy, Vol. 2, No. 2, 1988 (Pages 821-826)
Scanning Microscopy International, Chicago (AMF O'Hare), IL 60666 USA

0891-7035/88$3.00+.00

TRANSIT TIME EFFECT ON VOLTAGE CONTRAST IN THE STROBOSCOPIC SCANNING ELECTRON MICROSCOPE

K. Nakamae,* H. Fujioka and K. Ura

Electron Beam Laboratory, Faculty of Engineering
Osaka University, Yamada-Oka, Suita
Osaka 565, Japan

(Received for publication March 16, 1987, and in revised form November 23, 1987)

Abstract

Voltage contrast varies if the specimen voltage changes within the secondary electron transit time through the specimen electric field. This effect would affect the time resolution in stroboscopic scanning electron microscopy. The method to calculate the transit time effect that was described in a previous paper is reviewed. The calculated results agreed well with the experiment in which a specially designed specimen is used to estimate the applied voltage as exactly as possible.

Key Words: Transit time effect, Voltage contrast, Stroboscopic scanning electron microscope.

*Address for correspondence
K. Nakamae
Electron Beam Laboratory, Faculty of Engineering
Osaka University, Yamada-Oka, Suita
Osaka 565, Japan
Phone No. 06-877-5111, Ex. 4154

Introduction

It is well known that the time resolution of the stroboscopic scanning electron microscope is determined by the pulse width of the primary electron beam and the accuracy of synchronization between pulsed beams and the periodic device excitation. When the specimen voltage changes very fast, however, the secondary electrons suffer the effect due to the variation in the electric field: the voltage contrast variation rises. This transit time effect (TTE) affects also the time resolution in stroboscopic scanning electron microscopy. We have reported an analysis for the TTE (Fujioka et al., 1985).

In this paper, we shall try to compare the analysis with the experiment quantitatively. The specimen specially designed to estimate the applied voltage at the measured point as precisely as possible is used in the experiment. At first, we review the calculation method for the TTE.

Calculation Method

Since the purpose of this study is to compare the calculation with the experiment quantitatively, we review a calculation procedure (Fujioka et al., 1985) briefly. In the calculation, assumptions are: (1) a potential distribution above the specimen surface and motion of electrons are two-dimensional; (2) the experimental energy distribution of secondary electrons for metals by Kollath (1956) is approximated by the following:

$$N(W) = 1.5W \exp[2-(8W/3)^{1/2}] \tag{1}$$

(3) the angular distribution of secondary electron emission obeys Lambert's cosine law; (4) the electric field is quasi-static; (5) the size of the secondary electron emission area is very small; (6) the grid meshes in the spectrometer are fine enough; (7) the stray magnetic field from the SEM objective lens is neglected, and (8) the contribution of the secondary electrons generated by the backscattered electrons at the grid meshes is neglected.

The calculation model is assumed as shown in Fig. 1(a), which is the cross-section of the experimental specimen shown in a later section. The center of the measured electrode wire is set on the middle plane between the extraction grid and the ground electrode. V_S and V_E are voltages on the measured electrode and the secondary electron extraction electrode, respectively. A sinusoidal wave is applied to the measured electrode.

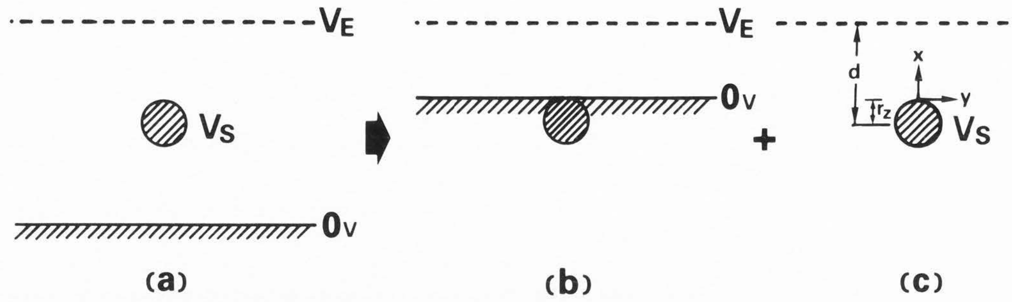

Fig. 1. Model of calculation. The potential distribution in (a) is approximated by superposing potential distributions in (b) and (c).

The potential distribution $\psi(x,z)$ in Fig. 1(a) is approximated by superposing the distributions in Figs. 1(b) and 1(c). Fig. 1(b) shows the electrode arrangement which has the grounded plane electrode on the top of the wire and the extraction grid. Fig. 1(c) is the arrangement which has the measured electrode wire and the grounded plane electrode. The potential distribution in Fig. 1(c) is given by Prinz (1969). Then,

$$\psi(x,z,t) = V_E z/(d-a) + V_S \log\left([(u-R)^2+v^2]^{1/2}/R\right)/\log(r/R)\,\sin(\omega t)$$

with (2)

$$u = [1/(R+r)-z] \,/\, ([1/(R+r)-z]^2+x^2\,)$$
$$v = -\,x/([1/(R+r)-z]^2+x^2)$$
$$R = 1/[2(d^2-a^2)^{1/2}] \qquad (>0)$$
$$r = [-1+d/(d^2-a^2)^{1/2}]/(2a) \qquad (>0)$$

The motion of an electron is determined by the following equations:

$$d^2x/dt^2 = e/m\cdot\partial\psi(x,z,t)/\partial x$$
$$d^2z/dt^2 = e/m\cdot\partial\psi(x,z,t)/\partial z \qquad (3)$$

Where, the initial conditions are,

$$t = t_0,\ x = z = 0$$
$$dx/dt = (2eW/m)^{1/2}\cos\alpha \qquad (4)$$
$$dz/dt = (2eW/m)^{1/2}\cos\alpha$$

e and m are the charge and mass of the electron, and eW and α are the initial energy and ejection angle of an emitted secondary electron.

The equation of motion is solved for the electron ejected at a certain stroboscopic phase with eW and α, using the Runge-Kutta-Gill method to describe the acceptance diagram, i.e., the area of (eW,α) accepted by the secondary electron detector. The current I collected by the detector is calculated as follows:

$$I = \iint N(W)\cos\alpha\; dW\, d\alpha \qquad (5)$$

The integration is performed with respect to the variables W, α, contained in the acceptance diagram (Nakamae et al., 1981). The detected currents are calculated as a function of the initial stroboscopic $\omega t_0 = \theta_0$ $(0 \leq \theta_0 \leq 2\pi)$: the stroboscopic waveform is obtained. Fig. 2 shows an example of calculated stroboscopic waveforms in the case of diameter 1 mm.

Experiment

The arrangement of the stroboscopic scanning electron miscroscope system is shown in Fig. 3. The system has a phase-shifter unit controlled by a minicomputer which allows the total delay of 1.6 ns in steps 0.0793 ps within an increment accuracy of 0.1 ps (Fujioka et al., 1986). For voltage measurement, a hemispherical retarding field energy analyser (Nakamae et al., 1985) is used.

Specimen

Fig. 4 shows the specimen arrangement. It is chosen for the following reasons:

(1) the applied voltage to the measured electrode can be easily estimated,

(2) there are no insulators near the measured electrode, which ensure that the disturbance in voltage distribution due to the charging up is minimized.

Estimation of applied voltage

The measured position is chosen at the distance 5 mm (L_1) from the open end of the measured electrode to avoid the disturbance of the electric field near both ends of the electrode. The applied voltage V_S at the measured position is calculated by the transmission line theory as follows:

$$V_S = 2\,2^{1/2}\,|\cos\phi|\,(PZ_0)^{1/2}\cos(\beta L_1)\,\sin(\omega t-\phi)\,/\,\cos(\beta L) \qquad (6)$$

L : measured electrode length
L_1 = 5 mm: distance from open end of measured electrode
$\phi = \tan^{-1}[Z_0\tan(\beta L)/Z_1]$
$\beta = 2\pi/\lambda$: phase constant
Z_0 : characteristic impedance of transmission line (50Ω)
Z_1 : characteristic impedance of measured electrode.
P : power of incident wave

The characteristic impedance of measured electrode Z_1 is decided by the measurement of standing waves. Thus the applied voltage on the measured position can be estimated by the power of incident wave. The impedance mismatch in the stroboscopic system estimated by VSWR is within 1.25 and the change in insertion loss of the phase shifter (see Fig. 3) is ±0.13 dB. As

② 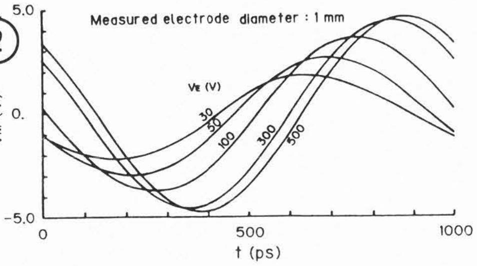

④ 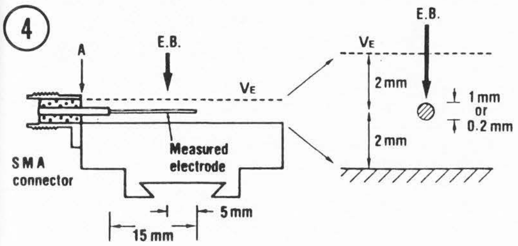

Fig. 2. Example of calculated stroboscopic waveforms as a parameter of the extraction voltage V_E. The diameter of measured electrode is 1 mm.

Fig. 4. Specimen arrangement. E.B. represents electron beam irradiation point.

a power meter and a power sensor combination, HP 435A (uncertainty ±0.1 dB) and HP 8481 (maximum VSWR 1.20) were used. Thus the uncertainty due to the power measurement instrument and the impedance mismatch is estimated as ±0.19 dB. Adding the change of 0.13 dB in the insertion loss to ±0.19 dB, the uncertainty in power measurement becomes ±0.32 dB. In terms of voltage, the uncertainty in estimation of applied voltage is ±4%.

Experimental conditions

Experimental conditions are shown in Table 1. A sinusoidal wave (1GHz) of $P = 62.5$ mW ($V_{in} = 2.5$ V) was applied to the measured electrode. On the measured electrode, the standing wave with a peak amplitude of about 5 V results. The diameters of the measured electrode were 1 mm and 0.2 mm.

Experimental results

Fig. 5 shows the measured waveform in the case of diameter 1 mm. The abscissa is the phase and the ordinate is the measured voltage. From this figure, as the extraction field is reduced, that is, the transit time becomes long, the peak amplitude of measured waveform is reduced and the phase is accordingly shifted.

Fig. 6 shows the peak-to-peak voltage V_{pp} of the measured waveform and the phase change $\Delta\Theta$ as a function of V_E. Where, V_{pp} is calibrated with the results of DC measurement and $\Delta\Theta$ is expressed in values at O V relative to one at $V_E = 500$ V. In this figure, the calculated results are also shown. It is seen that experimental results are well predicted by the calculation.

③ 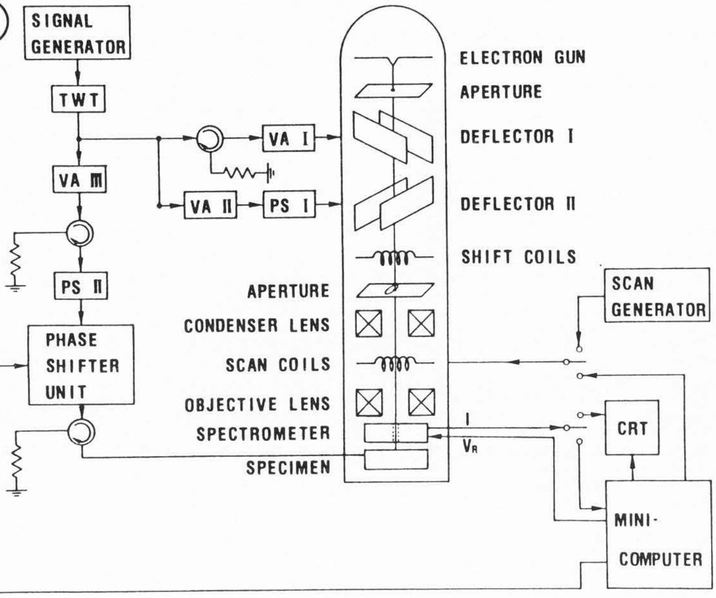

Fig. 3. Arrangement of the stroboscopic scanning electron microscope. TWT, VA, and PS represent travelling wave tube amplifier, variable attenuator, and phase shifter, respectively.

Table 1. Experimental Conditions

Beam accelerating voltage	5 kV
Peak beam current	7.2 nA
Applied signal frequency	1 GHz
Beam pulse width	20 ps
Applied input signal power	62.5 mW
Phase step width	10 ps
Number of phase steps	100
Number of signal averaging operations	10

It is also seen from this figure that the TTE for the measured electrode diameter of 1 mm is less than that for 0.2 mm. The specimen electric field extends up to the extraction grid as shown in Fig. 7 (Fig. 7 shows the potential distribution): the distance in which secondary electrons pass through becomes longer as the diameter of the wire is reduced. This is why the TTE for the diameter of 0.2 mm is greater than that for 1 mm.

Conclusions

Amplitude reduction and phase shift due to the TTE has been calculated and compared with the measurement: close agreement between calculation and experiment was obtained.

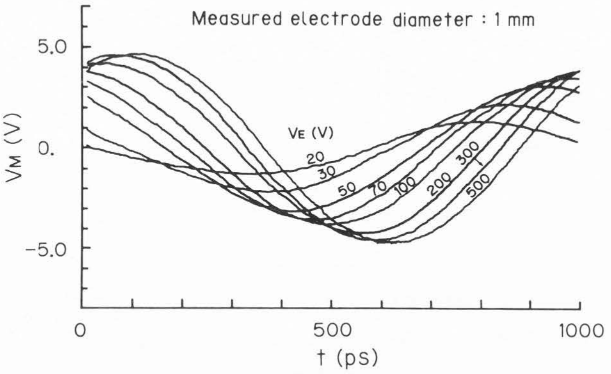

Fig. 5. Example of measured stroboscopic waveforms as a parameter of the exraction voltage V_E. The diameter of measured electrode is 1 mm.

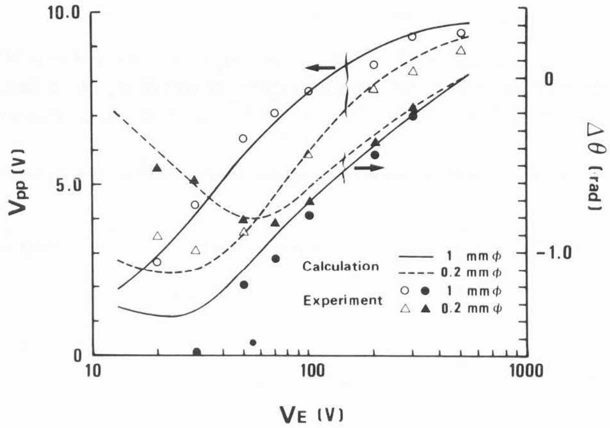

Fig. 6. V_{pp} and $\Delta\Theta$ as a function of V_E.

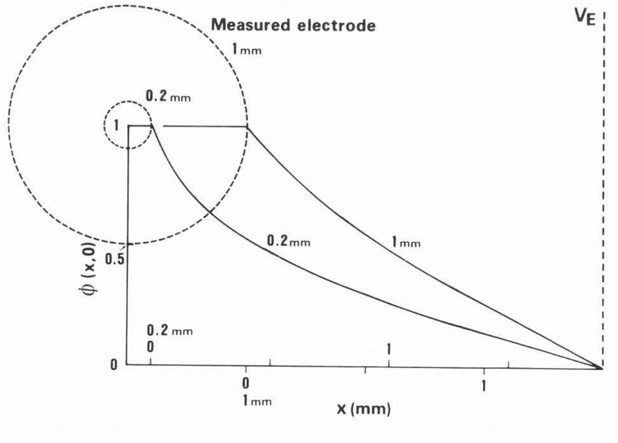

Fig. 7. Potential distributions on the z axis (x=0) as shown in Fig. 3 (V_S = 1 V).

Acknowledgments

This research was supported by the Special Budget – Joint Research between University and Industry – of the Ministry of Education, Science and Culture, Japan.

References

Fujioka H, Nakamae K, Ura K. (1985). Analysis of the transit time effect on the stroboscopic voltage contrast in the scanning electron microscope, J. Phys. D: Appl. Phys., **18**, 1019–1027.

Fujioka H, Kunizawa H, Ura K. (1986). 0.1 ps resolution delay circuit for waveform measurement in the stroboscopic scanning electron microscope, J. Phys. E: Sci. Instrum., **19**, 1025–1026.

Kollath R. (1956). Electronen-Emission Gasentladungen, Handbuch der Physik, **21**, 241.

Nakamae K, Fujioka H, Ura K. (1981). Local field effects on voltage contrast in the scanning electron microscope, J. Phys. D: Appl. Phys., **18**, 1939–1960.

Nakamae K. Fujioka H, Ura K. (1985). A new hemispherical retarding field energy analyzer for quantitative voltage measurements in the SEM, J. Phys. E: Sci. Instrum., **18**, 437–443.

Prinz H. (1969). Hochspannungsfelder, R. Oldenbourg Verlag Munchen Wien.

Discussion with Reviewers

K.A. Jenkins: The specimen tested has little resemblance to the circuits studied in most E-beam testing situations, namely, narrow lines (a few microns) close to a ground plane, with an extraction grid 1 or 2 mm above the surface. Your previous theoretical papers have dealt with these kinds of circuit. Have you done any corresponding experiment?
Authors: Yes, we are now making an experiment.

K.A. Jenkins: Have you convoluted the beam pulse width into the calculated waveforms?
Authors: Yes, but the effect of the beam pulse width on the waveform measurement is less than 1% in this experiment.

K.A. Jenkins: Have you measured at other frequencies, so that the results could be transformed into the time domain?
Authors: We have not tried it as yet.

A.R. Dinnis: The approximation to the field distribution indicated in Fig. 1 seems rather crude. Can you comment on the accuracy of the approximation and on how much it will affect the calculated results?
Authors: We have checked the potential distribution by using a finite difference method. The difference is 10% at the most.

L. Kotorman: What material is the sample (wire) made of, and what type of surface preparation has been performed? (I am referring to possible localized surface charging even on metal samples as reported by many).
Authors: The wire is made of copper and polished chemically.

L. Kotorman: Is the 5 keV beam preferable for this measurement, what is the reason for not using lower energy? How significant is the collected back-scattered current in relation to the secondary electron current, and can it be disregarded?
Authors: It was only to improve the SN ratio. We use a hemispherical retarding-field energy analyser with a microchannel

Table 2. Examples of calculated TTE for integrated circuit geometries.

No	2a(μm)	T(ps)	E(V/mm)	2a/T(μm/ps)	Θ_E	τ_+/T
1	10	100	500	0.1	0.15	0.10
2	1	100	500	0.01	0.048	0.02
3	1	10	500	0.1	0.48	0.14
4	1	10	50	0.1	1.5	0.15

plate detector (MCP). The hole is made in the center of the MCP to pass the primary electrons and is 5.6 mm in diameter (Nakamae et al., 1986): we expect that the effect of back-scattered electrons is not so much.

L. Kotorman: Using the experimental conditions given, I estimate the mean throughput during the 20 picosec. as about one electron. How many beam enable pulses are needed to produce a meaningful measurement on one spot of the waveform and how many spots are needed to produce the whole waveform?
Authors: The number of some hundred beam enable pulses are sufficient to produce a meaningful measurement in respect to SN ratio. The waveform is composed of 100 phase points.

L. Kotorman: How could you determine the beam pulse width as of 20 pico seconds? What would you estimate for time spread of the primary beam at the sample ?
Authors: In the region where the longitudinal velocity spread introduced in the deflection system does not significantly influence the pulse width, the pulse width can be simply estimated by measuring the ratio of average (chopped) to peak (unchopped) beam current. Here we have used this method. Calculation shows that the time spread is several picoseconds.

L. Kotorman: What are the physical dimensions of "Deflector I" and "II" plates? How would the transit time between these plates pose limitations for the measurements?
Authors: Please refer to the paper by Ura et al. (1978).

L. Kotorman: Could you please give the size of the beam choping aperture?
Authors: The final aperture image acts as a chopping aperture and its size is about 100 μm in the experimental condition.

L. Kotorman: What is the pause time between the 20 ps beam pulses? What kind of amplifier system are you using in conjunction with your analyzer?
Authors: The pause time is 980 ps. Our amplifier system is composed of a microchannel plate detector, a current-to-voltage converter and amplifier circuits (Nakamae et al., 1986).

L. Kotorman: It appears that the reported calculations and measured results could be very useful to determine "TTE" limitations when testing certain samples stroboscopically (for example, microwave components with compatible geometries). However, the physical dimensions of the sample used here and its separation from the ground plane are a thousand fold greater than a typical micro-circuit element. If my estimation is right concerning a field effect curve corresponding to integrated circuit dimension on Figure 7, the TTE would extend only a few micrometers above the sample and would be insignificant beyond that all the way to the extraction grid. Am I correct when suggesting that the TTE for integrated circuits would be less significant than the values reported here and, therefore, are of no serious concern at least for electric field type analyzers?

W. Reiners: If I understand it correctly, the TTE for the diameter of 0.2 mm of the measured electrode is greater than that for 1 mm, because the way of the secondary electrons through the electric field which exists between electrode and extraction grid is longer in the case of 0.2 mm. However, for real line geometries with line spacings and widths in the order of 0.5–10 μm the electric field has only an extension in the same order. Thus TTE reduces for smaller line geometries. Could the TTE, therefore, be neglected for future designs of integrated circuits?
Authors: If only the measured electrode width is reduced but the secondary electron extraction field and the time variation in the waveform on the measurement electrode are not changed, the TTE for integrated circuits reduces. But when the extraction field or the time variation is changed, the TTE cannot be always disregarded.

It can be demonstrated that the stroboscopic voltage contrast is a function of three parameters. Here a step function with a peak voltage V_S and a rise or fall time of T is supposed to be applied on the measurement electrode in an integrated circuit. T corresponds roughly to the reciprocal of input signal frequency. The electrode width and the distance between electrodes are the same and equal to 2a. The secondary electron extraction field is E. We take Θ_E, V_S, and $E \cdot 2a$ as parameters. Θ_E is the transit angle in which an electron with an initial energy O eV reaches the point at distance 2a from the electrode through the extraction field E. It is defined by $2(2a/T)/\sqrt{(2e/m)(E \cdot 2a)}$. Examples of the calculated TTE for integrated circuit geometries are shown in Table 2, where V_S is assumed to be 5 V. τ_+ indicates the degree of waveform distortion and defined in the paper by Fujioka et al. (1985). This shows that the TTE (τ_+/T) is reduced as Θ_E decreases. Even if the width 2a is reduced from 10 μm to 1 μm, the TTE increases with decreasing the rise time T (compare No. 1 to No. 3). Furthermore, when the extraction field is reduced, the TTE increases (compare No. 3 to No. 4). Thus whether the TTE for integrated circuit geometries can be disregarded or not depends on not only the measurement electrode width but also the time variation T and the extraction field E.

W. Reiners: You show that TTE can theoretically be calculated for a certain measurement electrode arrangement. Thus it should be possible to determine TTE also for real line geometries. Is there a chance to reconstruct the real waveform at a line from the measured waveform? If not, could the measured waveform be improved (with less distortion caused by TTE)?
Authors: We think that the TTE can be corrected by calculations if the specimen electrode structure and the potential distribution are known.

Additional references

Nakamae K, Fujioka H, Ura K, Takagi T, Takashima S. (1986). A hemispherical retarding-field energy analyser with a microchannel plate detector and a high extraction field for voltage measurement in the scanning electron microscope, J. Phys. E: Sci. Instrum., **19**, 847–852.

Ura K, Fujioka H, Hosokawa T. (1978). Electron optical design of picosecond pulse stroboscopic SEM. In: Scanning Electron Microsc. 1978; I: 747–753.